

# Cross-Strand Interactions of Fluorinated Amino Acids in $\beta$ -Hairpin Constructs

Ginevra A. Clark,<sup>†,§,⊥</sup> James D. Baleja,<sup>\*,‡,§</sup> and Krishna Kumar<sup>\*,†,§</sup>

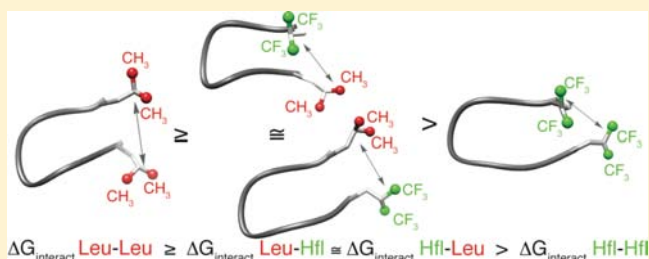
<sup>†</sup>Department of Chemistry, Tufts University, 62 Talbot Avenue, Medford, Massachusetts 02155, United States

<sup>‡</sup>Department of Biochemistry, Tufts University School of Medicine, Boston, Massachusetts 02111, United States

<sup>§</sup>Cancer Center, Tufts Medical Center, Boston, Massachusetts 02111, United States

## Supporting Information

**ABSTRACT:** We describe herein the design, synthesis, and thermodynamic characterization of fluorinated  $\beta$ -hairpin constructs. Introduction of hexafluoroleucine (Hfl) did not perturb  $\beta$ -hairpin formation, as judged by <sup>1</sup>H NMR structures of four peptides determined to <1 Å backbone RMSDs, allowing direct comparison of thermodynamic stabilities of fluorinated peptides to their hydrocarbon counterparts. Judicious fluorination of peptides often results in increased thermal and chemical stability of the resultant folded structures. However, we found that when cross-strand residue partners were varied, the side-chain interaction energies followed the order Leu-Leu > Hfl-Leu > Hfl-Hfl. All peptides were more structured in 90% MeOH than in aqueous buffers. The peptides with Hfl-Leu or Hfl-Hfl cross-strand partners showed increased interaction energies in this solvent compared to those in water, in contrast to the insignificant effect on Leu-Leu. Our results inform the binding and assembly of peptides containing Hfl in the context of  $\beta$ -sheet structures and may be useful in interpreting binding of fluorinated ligands and peptides to biological targets.



## INTRODUCTION

About a fifth of the drugs on the market and about a third of agrochemicals contain the element fluorine.<sup>1</sup> Fluorine has intrigued chemists and biologists because of its unique properties and a near complete absence in soft tissue.<sup>2,3</sup> Carbon-bound fluorine continues to resist being boxed into usual parametric molecular modeling programs. Therefore, a detailed understanding of the interactions of fluorinated molecules with biological targets remains an active area of research.

Fluorination modulates the properties of lipids,<sup>4</sup> pharmaceuticals,<sup>1</sup> and peptides,<sup>5</sup> where dramatic differences are observed depending upon the degree of fluorination. Fluorocarbons have exceedingly low polarizabilities for their size and, hence, have lower interaction energies than hydrocarbons.<sup>6,7</sup> The difference in interaction energy relative to size has been used to explain the immiscibility of hydrocarbons and fluorocarbons. However, it is not clear how this property relates to fluorinated amino acids in folded peptides, which have a lower degree of fluorination. The influence of fluorination on the transition temperature of vesicles from gel to liquid crystal phase, an indicator of increased interactions, has been investigated. In derivatives with fewer than five perfluorinated carbons the transition temperature decreases. However, with at least eight perfluorocarbons, the transition temperature increases.<sup>4,8</sup> It has been suggested that as the length of the fluorinated chain increases, its low cohesion is offset by increased hydrophobicity. It is worthwhile to note that, while

perfluorination leads to molecules that are highly nonpolar, monofluorination can lead to dipolar interactions.<sup>9</sup> Studies that directly compare the interaction of trifluoromethyl groups with both hydrocarbon and fluorinated binding partners are therefore valuable.<sup>10,11</sup>

Protein folding in water is frequently driven by the hydrophobic effect; therefore, increasing the hydrophobicity of an interior residue usually increases the stability of a folded structure.<sup>12</sup> This has been effectively achieved by the substitution of a methyl group with a trifluoromethyl group.<sup>10,11,13–19</sup> The hydrophobic effect is based on the principle that nonpolar surfaces cannot compete with the strong attraction of water for itself and are driven out of solvent.<sup>12</sup> This principle applies equally to fluorinated and hydrocarbon groups. For example, the binding affinity to carbonic anhydrase was correlated to the surface area of the hydrophobic tail for cyclic, branched, and fluorinated ligands.<sup>20</sup> When normalized for surface areas, the hydrophobicities of hydrocarbons and fluorocarbons are similar.<sup>20</sup> This has also been observed with highly fluorinated coiled coil systems and  $\beta$ -peptide assemblies.<sup>21</sup> More recent studies have examined the role of both hydrophobic surface area and inductive effects on the properties of ligands or proteins. In addition to their enhanced hydrophobic surface area, strongly electron-withdrawing fluorinated pendant groups perturb the Lewis basicity

Received: December 26, 2011

Published: October 18, 2012

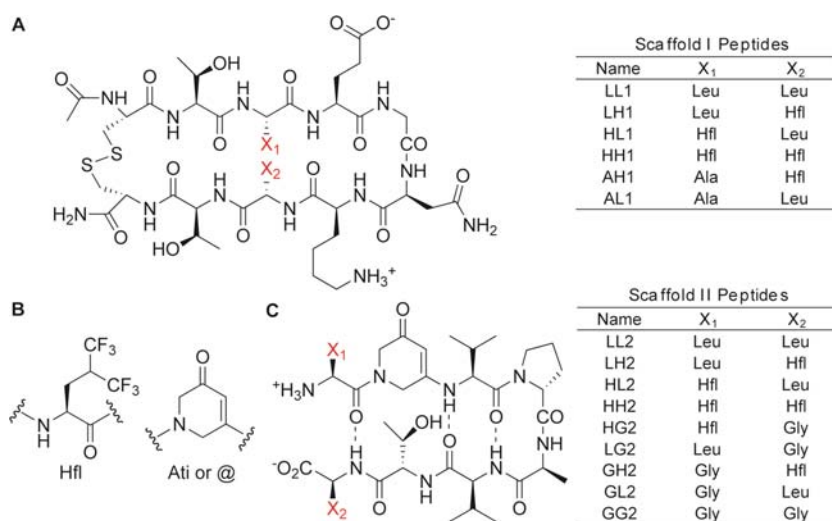


**Figure 1.** Structures of scaffolds I and II peptides. (A) Variants LL1 through AL1 were prepared to examine scaffold I. (B) Molecular structures of Hfl and Ati (or single-letter code “@”). (C) Variants LL2 through GG2 were prepared to examine scaffold II. Substitutions were made at positions X<sub>1</sub> and X<sub>2</sub> (in red). For scaffold II, additional control folded and unfolded peptides were prepared with the sequences Val-Ati-Thr and Cys = Val-<sup>19</sup>Pro-Ala-Val-Ati-Val-<sup>19</sup>Pro-Ala-Val-Val (cyclic), respectively.

or hydrogen-bonding interactions of proximal functional groups.<sup>22,23</sup> In previous studies, either the ligand or the protein was fluorinated, but not both. Herein, we have evaluated differences in the interactions of fluorinated and nonfluorinated compounds with both fluorinated and nonfluorinated binding partners.

Studies in our laboratory and others have focused on substituting Leu and Hfl into the core of peptides and proteins containing the coiled coil motif. However, in such constructs, stabilities are intimately linked to packing, and the oligomerization state. Marsh and co-workers observed that, in aqueous medium, Hfl (substituted at only one hydrophobic packing layer, therefore not “fluorous”) and Leu-substituted antiparallel 4-helix bundles form heterodimers and suggested that fluorination does not lead to the segregation of fluorinated peptides from their hydrocarbon counterparts.<sup>24</sup> However, we have previously demonstrated that in a different construct, Hfl-substituted coiled coils and Leu-substituted coiled coils strongly favor homodimer formation.<sup>10</sup> In order to explore the interactions of Hfl in hydrophobic environments, Bilgiçer et al. substituted the core residues of a coiled coil motif with either Leu or Hfl, while the exterior residues were substituted with hydrophobic amino acids.<sup>13</sup> The presence of the hydrophobic amino acids leads to partitioning of the peptides into micelles, and peptides substituted with Hfl aggregated into higher-order assemblies.<sup>13</sup> These results showed that Hfl-substituted peptides oligomerize in the nonpolar context of membranes. In the coiled coil motifs described, 6–12 Hfl residues were incorporated into each peptide chain, resulting in oligomerized constructs containing 14–48 Hfl residues at the interface. Thus, these represent highly fluorinated systems.

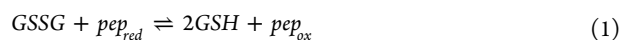
We report here constructs with only one or two Hfl residues that allow quantitative evaluation of Hfl-Hfl and Hfl-Leu interactions. The degree of fluorination, as well as the environment, organic versus aqueous solution, influences the interactions of fluorinated amino acids. We report here a system designed to determine interaction energies of Leu and Hfl (hexafluoroisoleucine) side chains and dissect factors that contribute to the conformational stability of peptides.<sup>25,26</sup> In addition, the envisaged constructs also allow evaluation of the

extent to which fluorination stabilizes or destabilizes  $\beta$ -hairpin motifs.<sup>27–29</sup> While much information has been gleaned from the  $\alpha$ -helical coiled coil systems previously studied,<sup>10,11,13–19,21</sup> we sought to incorporate fluorinated amino acids into a simpler scaffold ( $\beta$ -hairpins), allowing for facile synthesis and characterization. Such systems have been previously used to evaluate interaction energies and therefore provide a database for comparison. For instance, aromatic,<sup>30</sup>  $\pi$ -cation,<sup>31</sup> and hydrophobic<sup>32</sup> interactions have been quantified using various  $\beta$ -turn scaffolds. Furthermore,  $\beta$ -hairpins can inhibit protein–protein interactions,<sup>33–36</sup> bind specifically to ssDNA,<sup>37,38</sup> and potentially serve as lead compounds for drug discovery. We studied cross-strand interactions in two complementary scaffolds. In one scaffold, developed by Cochran, we interrogated interactions at non-hydrogen-bonded residues,<sup>39,40</sup> and in another, reported by Bartlett, we analyzed interactions between residues located at the free N- and C-termini.<sup>41–44</sup> These results provide insight into how fluorine influences interactions between biological molecules—an important factor in drug design.<sup>1,45</sup>

## EXPERIMENTAL SECTION

**Synthesis.** Synthesis of amino acids and peptides, purification procedures, and characterization are included in the Supporting Information (SI). A description of reagents, preparation of stock solutions, and buffers is also included.

**Determination of  $C_{eff}$  for Scaffold I Peptides.** The disulfide-bonded scaffold I peptides were allowed to undergo thiol exchange in a mixture of oxidized and reduced glutathione where:



GSH and GSSG are reduced and oxidized glutathione, respectively, and  $\text{pep}_{red}$  and  $\text{pep}_{ox}$  are reduced and oxidized peptides, respectively. The stability of the scaffold I constructs was evaluated by comparing  $C_{eff}$  values for each peptide, where:<sup>39,40</sup>

$$C_{eff} = \frac{[\text{pep}_{ox}][\text{GSH}]^2}{[\text{GSSG}][\text{pep}_{red}]} \quad (2)$$

Higher  $C_{eff}$  values indicate that more of the peptide is in the folded form. The ratio of oxidized to reduced peptides was determined at 20 °C, pH 8.1, and quantified by HPLC. We examined  $C_{eff}$  at 375, 37.5,

and 18.75  $\mu\text{M}$  peptide concentrations. In order to evaluate the constructs,  $C_{\text{eff}}$  at 18.75  $\mu\text{M}$  peptide concentrations was converted to  $\Delta G$ , where:

$$\Delta G = -RT \ln C_{\text{eff}} \quad (3)$$

The  $\Delta G$  values are for the reaction shown in eq 1. Note that the  $\Delta G$  of folding cannot be directly measured, as  $C_{\text{eff}}$  is also a function of glutathione concentrations. Detailed experimental procedures at each concentration are provided in the SI.

**Scaffold II: Determination of Fraction Folded ( $\chi_{\beta}$ ).** In order to evaluate the stability of the peptides prepared with scaffold II, CD spectra from 320 to 240 nm were obtained at 15, 37.5, and 60  $\mu\text{M}$  concentrations in 10 mM phosphate buffer, pH 7.0, 25  $^{\circ}\text{C}$ . Raw CD data at 282 nm were converted to molar ellipticity  $[\theta]_{\text{obs}}$  in  $\text{deg}\cdot\text{cm}^2/\text{dmol}$  using eq 4:<sup>42</sup>

$$[\theta]_{\text{obs}} = 10^5 \frac{\theta_{\text{raw}}}{[\text{peptide}(\mu\text{M})]} \quad (4)$$

where the CD signal at 282 nm was attributed exclusively to the Ati residue (1,2-dihydro-3(6H)-pyridinone) (Figure 1). Ati may be referred to by its single-letter amino acid code “@” (Figure 1). Molar ellipticities were converted to fraction  $\beta$ -turn ( $\chi_{\beta}$ ) using the following equation:

$$\chi_{\beta} = \frac{[\theta]_{\text{obs}} - [\theta]_0}{[\theta]_{100} - [\theta]_0} \quad (5)$$

The molar ellipticity for the unfolded state,  $[\theta]_0$ , was obtained from the linear tripeptide “V@T” ( $-2.62 \times 10^4 \text{ deg}\cdot\text{cm}^2/\text{dmol}$ , see SI). The molar ellipticity for the fully folded state,  $[\theta]_{100}$ , was obtained from the cyclic control peptide (Cyc, Figure 1) ( $-19.96 \times 10^4 \text{ deg}\cdot\text{cm}^2/\text{dmol}$ , see SI). The CD spectra showed no change in molar ellipticity over the concentration range studied (15 to 60  $\mu\text{M}$ ) suggesting that the construct is monomeric in the range studied. We believe this species to be a monomer, based on literature precedence, and our NMR studies on four of the peptides in 30% MeOH at 1 mM peptide concentrations. In order to improve the statistical significance of the data,  $\chi_{\beta}$  was measured five times for each peptide at 15  $\mu\text{M}$  peptide concentrations. The free energies of folding ( $\Delta G^{\circ}_{\text{XY}}$ , Figure 3A) were obtained using the following equation:

$$\Delta G^{\circ}_{\text{XY}} = -RT \ln \left[ \chi_{\beta} / (1 - \chi_{\beta}) \right] \quad (6)$$

Similar procedures were used to determine  $\Delta G^{\circ}_{\text{XY}}$  in 90% MeOH and 60% trifluoroethanol (TFE). Detailed experimental procedures are provided in the SI.

#### Scaffold II: Temperature-Dependent CD Measurements.

Variable temperature data in aqueous solutions were collected at 5  $\mu\text{M}$  concentrations from 5 to 95  $^{\circ}\text{C}$  and monitored at 282 nm. Variable temperature data in mixed organic/aqueous solutions were collected from 5 to 60  $^{\circ}\text{C}$ . Additional experimental details, denaturation curves, and a description of the thermodynamic analysis performed are provided in the SI.

#### Scaffold II: Determination of Peptide Structure by NMR.

Detailed experimental procedures and calculations are provided in the SI. Briefly, two-dimensional (2D) NMR experiments on scaffold II peptides were performed in 30%  $\text{CD}_3\text{OD}$  at pH 7.0 on a Bruker AMX-500 spectrophotometer. Two-dimensional ROESY spectra were collected for each peptide with 100 ms mixing times. Additional ROESY, NOESY, COSY, and TOCSY spectra were collected as described in the SI. Spectral assignments were made as described in the SI. Restraints and additional parameter files were developed and input into *CNSsolve* v1.1<sup>46</sup> for structural refinement, as described in the SI.

## RESULTS

**Construct Design.** We surveyed the scaffolds previously used to study interaction energies, and chose scaffolds I and II that were synthetically tractable.<sup>39,41–44,47,48</sup> Cochran and co-

workers identified a relatively short and stable  $\beta$ -turn construct<sup>47</sup> (scaffold I; Figure 1A). The hairpin turn is promoted by a Gly-Asn sequence, and the N and C-terminal Cys residues form a disulfide bond, stabilizing the hairpin. They determined the hairpin stability of a series of variants by measuring the extent of disulfide bond formation ( $C_{\text{eff}}$ ) between the terminal cysteine residues in a redox-controlled environment.<sup>40</sup> It was reasoned that hairpin formation would position the terminal residues to be proximal promoting the formation of a disulfide bond. The  $C_{\text{eff}}$  values were correlated with  $H_{\alpha}$  chemical shift values for several residues, establishing that increased  $C_{\text{eff}}$  corresponds with increased  $\beta$ -hairpin stability. Cochran and co-workers systematically substituted the amino acids at interacting residues 3 and 8 ( $X_1$  and  $X_2$ ; Figure 1).<sup>40</sup> The backbone atoms of these residues are not engaged in H-bonding, so any changes in interaction energies are a direct result of side-chain interactions. In general, Cochran and co-workers observed that increasing the hydrophobicity of the  $X_1$  and  $X_2$  residues increased the stability of the turn.<sup>40</sup> We anticipated that substitution of Leu with Hfl at one or both positions would increase the  $\beta$ -turn propensity of the sequence due to the enhanced hydrophobicity of Hfl relative to Leu. However, it was unclear if Leu-Leu, Hfl-Leu, or Hfl-Hfl pairings would contribute to the stability of the hairpin in a synergistic manner. A series of variants with Leu, Hfl, and Ala substitutions (Figure 1A) were synthesized to evaluate these interactions. Leu and Hfl were substituted in all possible combinations, while Ala was substituted only at the  $X_1$  position. Peptide AL1 has alanine at  $X_1$  and leucine at  $X_2$ , where the remainder of the sequence is defined by scaffold I. Peptides LL1, LH1, HL1, HH1, and AH1 are named so that H in the peptide identifier stands for hexafluoro-leucine, while L and A stand for leucine and alanine (Figure 1A).

Bartlett and co-workers have developed a different construct (scaffold II) to quantify interactions between side chains in  $\beta$ -hairpins.<sup>41–44</sup> In this construct, the turn is promoted by a <sup>D</sup>Pro-Ala sequence. Introduction of an Ati residue restricts the flexibility of the backbone, leading to  $\beta$ -sheet stabilization (Figure 1B). Although Ati is able to engage in cross-strand H-bonds of the usual register, it lacks the ability to H-bond on the external face of the hairpin, mitigating oligomerization of the motif. Furthermore, UV absorption allows for detection of the folded state by monitoring of the CD signal at 282 nm.<sup>41,42</sup> This provides a technical advantage, since natural  $\beta$ -turn peptides are generally only modestly stable in aqueous solution. A series of variants was prepared to study cross-strand interactions at the terminal positions ( $X_1$  and  $X_2$ ).<sup>41</sup> Hydrophobic residues were consistently preferred, and favorable side-chain–side-chain interactions were observed for hydrophobic residues. We envisioned that this system would reveal differences between Leu-Leu, Hfl-Leu, and Hfl-Hfl interactions. Furthermore, this system is amenable to thermal analysis, allowing determination of thermodynamic parameters that dictate folding. Constructs with Leu, Hfl, and Gly substitutions in all possible combinations were synthesized (Figure 1C). The peptide GL2 was composed of Gly at  $X_1$  and Leu at  $X_2$ , where the remainder of the sequence was defined by scaffold II. The peptides LL2, LH2, HL2, HH2, HG2, LG2, GH2, and GG2 were named according to the convention described previously (Figure 1C).

**Determination of Peptide Stabilities and Concentration-Dependent Effects.** For scaffold I peptides,  $C_{\text{eff}}$  was measured at 18.75, 37.5, and 375  $\mu\text{M}$  peptide concentrations.

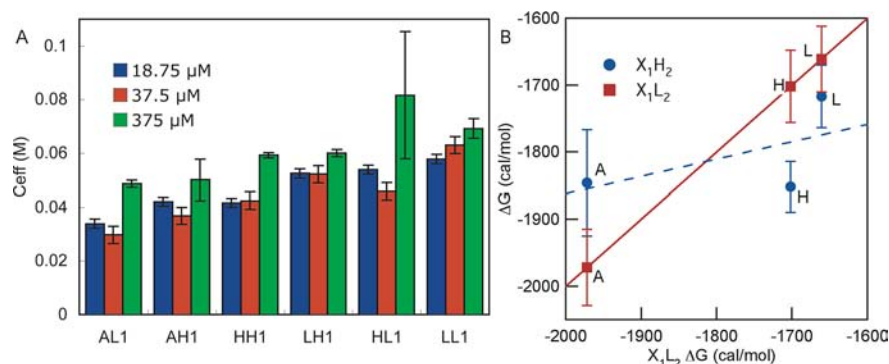


**Figure 2.** (A)  $C_{eff}$  values at 18.75, 37.5, and 375  $\mu\text{M}$  Peptide Concentrations. See SI for experimental conditions. At 18.75 and 37.5  $\mu\text{M}$ , error bars represent the 95% confidence interval from multiple comparison tests, where the data was collected from three independent experiments for a total of six HPLC traces. The error bars for experiments performed at 375  $\mu\text{M}$  represent the standard deviations of three independent experiments, where the average of five HPLC traces were used for each experiment. Uniformity of the data at 18.75  $\mu\text{M}$  and 37.5  $\mu\text{M}$  was determined using Bartlett's test ( $p = 0.05$ ). (B)  $\Delta G$  for glutathione–peptide disulfide exchange at 18.75  $\mu\text{M}$  peptide concentrations, scaffold I. Peptides with Hfl at  $X_2$  (blue circles,  $X_1\text{-Hfl}_2$  series) are plotted against the corresponding peptide that contains Leu at  $X_2$  (red squares,  $X_1\text{-Leu}_2$  series). The identity of the amino acid at the  $X_1$  position is indicated next to each point. The  $X_1\text{-Leu}_2$  series is plotted against itself (red squares) for reference. Error bars are the standard deviations.

At 375  $\mu\text{M}$  peptide concentrations, a slightly higher  $C_{eff}$  was observed for each peptide. Minor differences in  $C_{eff}$  at 375  $\mu\text{M}$  concentrations were expected, since a different concentration of the glutathione stock solutions was required for these experiments (see SI).  $C_{eff}$  for peptides at 375  $\mu\text{M}$  peptide concentrations for the nonfluorinated peptides was found to be in agreement with previous reports.<sup>39,40</sup> HL1 showed anomalously large  $C_{eff}$  and variability at 375  $\mu\text{M}$ , but behaved consistently at lower concentrations (Figure 2A).

For scaffold II peptides, thermodynamic parameters were extracted assuming a two-state model where the peptide is monomeric, and either fully folded (state 1) or unfolded (state 2). This model assumes that the unfolded state does not contribute to the CD signal that we are monitoring for the folded peptide. This model further assumes that, if present, partially folded states are at insignificant concentrations, or do not significantly affect the CD signal. These assumptions are consistent with the observation of cooperative stabilizing effects upon simultaneous mutation of the terminal or interior residues.<sup>41</sup> A two-state model is also consistent with 1-dimensional  $^1\text{H}$  NMR spectra of LL2 and LH2 in buffer, that showed two resonances for each amide proton in aqueous solution at ambient temperatures, and the  $^{19}\text{F}$  NMR spectrum of LH2, which showed two resonances for each trifluoromethyl group at ambient temperature (see SI). In aqueous solution, the observation of two signals for each amide is probably due to cis/trans isomerization of 3-Val-4-D-Pro amide bond.<sup>49</sup> The cis conformation of this bond provides the appropriate geometry for the turn sequence while the trans amide bond does not.<sup>49</sup> Thus, the observed cis/trans isomerization of this bond suggests that a proportion of the unfolded peptide was in the extended random coil conformation, whereas the folded peptide can only be formed upon isomerization.<sup>49</sup> In 30% MeOH at 283 K, one set of resonances was observed, consistent with a peptide in the favored cis conformation of the 3-Val-4-D-Pro amide bond.

In addition, for scaffold II peptides, no concentration dependence of the molar ellipticities was observed from 15–60  $\mu\text{M}$  concentrations in buffer. All NOESY crosspeaks in 30% methanol (1 mM peptide) could be accounted for, assuming a monomeric species. Together the data suggest a

single monomeric species in solution. Therefore,  $\Delta G_{XY}^\circ$  was calculated from  $\chi\beta$ , as determined by CD, according to eqs 5 and 6.

**Determination of  $\beta$ -Sheet Propensities for Hfl.**  $\beta$ -Sheet propensities are determined from the relative stabilities of constructs in which the side chains of interest do not interact with other side chains. Minor and Kim<sup>50</sup> found that  $\beta$ -sheet propensities for natural amino acids vary by  $\sim 2$  kcal/mol in a model based on the streptococcal protein G  $\beta 1$  domain ( $\beta 1$ -domain). They also demonstrated that  $\beta$ -sheet propensity increases in the series Ala, Val, Ile,<sup>50</sup> and propensities follow the same order for scaffold I<sup>40</sup> and scaffold II<sup>41</sup> peptides. These previously established correlations between  $\beta$ -sheet propensity and hydrophobicity suggest our model systems are appropriate. It is worthwhile to note that context plays a significant role in  $\beta$ -sheet propensities,<sup>51</sup> and indeed we observe that context influences the  $\beta$ -sheet propensities of Leu and Hfl. For scaffold I peptides, we found that AH1 was more stable than AL1 by 130 cal/mol at 18.75  $\mu\text{M}$  peptide concentration, suggesting that Hfl had only a slightly higher  $\beta$ -sheet propensity than Leu (Figure 2). Examination of the stabilities ( $\Delta G_{XY}$ ) of the Gly derivatives for scaffold II peptides (Figure 3A, peptides GL2, LG2, GH2, and HG2) showed that Leu and Hfl have similar  $\beta$ -sheet propensities, although the  $\beta$ -sheet propensity of Hfl was higher than that of Leu at the C-terminus, but lower than that of Leu at the N-terminus. In this case, the overall stability of scaffold II was more sequence-dependent, varying from 841 to 413 cal/mol. The basicity of the amino group of Hfl is 100-fold lower than that of Leu, reflecting an inductive effect of the  $\text{CF}_3$  groups on the  $\text{p}K_a$ <sup>52</sup> underscoring that electrostatic interactions between the N- and C-termini of the folded hairpin contribute to the overall stability. Since scaffold I peptides are substituted at non-hydrogen bonding positions, they should be less sensitive to electronic effects. Further, it is possible that diagonal interactions between the side chains at positions 1 (Leu or Hfl) and 6 (Val) are more favorable for Leu than for Hfl in scaffold II. Work by Gellman and co-workers has demonstrated that these diagonal interactions contribute to the overall stability of  $\beta$ -hairpins, and that this pairing is directional, based on the overall twist of the hairpin sequence.<sup>53</sup> Indeed, between residues 1 and 6 we observe two NOE crosspeaks for

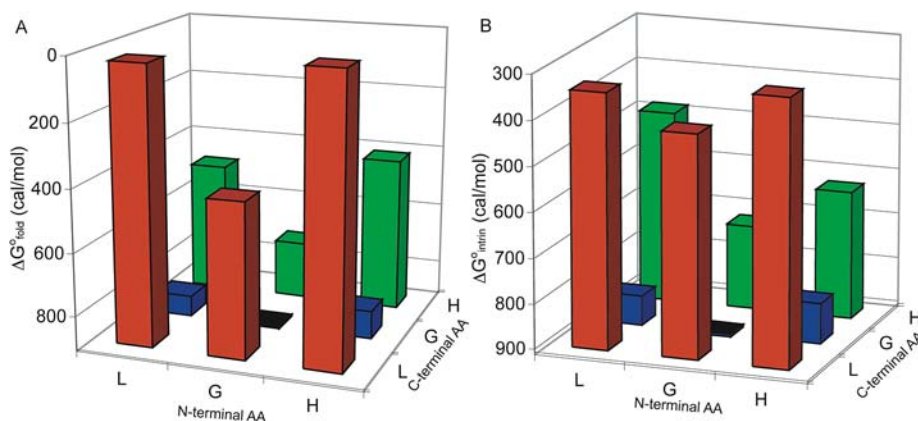


**Figure 3.** (A)  $\Delta G^{\circ}_{\text{fold}}$  for scaffold II peptides. (B)  $\Delta G^{\circ}_{\text{intrinsic}}$  for scaffold II peptides. Conditions: 15  $\mu\text{M}$  peptide, 10 mM phosphate buffer, pH 7.0, 25  $^{\circ}\text{C}$ . The baseline is set at 912 cal/mol, corresponding to the stability of GG2. Intrinsic stabilities were calculated using eq 7.

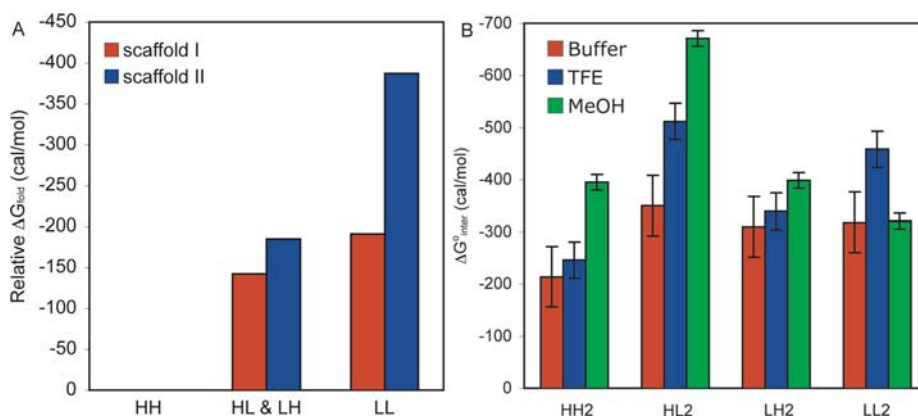


**Figure 4.** (A) Comparison of stabilities of scaffolds I and II. The stabilities relative to HH are shown. The average stability for the peptides substituted with both Hfl and Leu is shown. For both scaffolds, peptides substituted with Hfl at both  $X_1$  and  $X_2$  were the least stable. (B)  $\Delta G^{\circ}_{\text{interact}}$  for scaffold II peptides. Red, 15  $\mu\text{M}$  peptide, 10 mM phosphate buffer, pH 7.0, 25  $^{\circ}\text{C}$ . Blue, 15  $\mu\text{M}$  peptide, 40% 10 mM phosphate buffer, pH 7.0, 60% TFE, 25  $^{\circ}\text{C}$ . Green, 15  $\mu\text{M}$  peptide, 10% 10 mM phosphate buffer, pH 7.0, 90% MeOH, 25  $^{\circ}\text{C}$ . Error bars are the 95% confidence intervals from five independent measurements as determined using a multiple comparison test. Interaction energies were calculated using eq 8.

HH2 and HL2, three crosspeaks for LH2, and four crosspeaks for LL2. This suggests stronger 1–6 diagonal interactions for LH2 and LL2 than for HH2 and HL2.

Cheng and co-workers recently determined the  $\beta$ -sheet propensity of selected fluorinated amino acids by substitutions at residue 53 of the  $\beta 1$ -domain and examining the stability of the prepared constructs.<sup>27</sup> Substitutions at position 53 of  $\beta 1$  were more sensitive than scaffold I or scaffold II, nevertheless, the results of Cheng and co-workers are consistent with our observations. For example, substituting Ala for Leu at residue 53 of  $\beta 1$ -domain leads to  $\sim 1$  kcal/mol increase in stability, while a similar substitution on scaffold I provides only a 270 cal/mol increase. Taken together, these results demonstrate that propensities are dependent on sequence context and, in most instances, are higher for Hfl than for Leu. Raleigh and co-workers used a buried position and found that trifluorovaline provides even higher stability.<sup>27</sup>

#### Determination of Interaction Energies for Scaffold I.

Smith and Regan first demonstrated that side-chain interaction energies were significant in  $\beta$ -sheet folding in  $\beta 1$  model proteins.<sup>54</sup> Using a double mutant analysis, they observed interaction energies for aromatic and hydrophobic amino acids of  $\sim 0.2$ – $0.6$  kcal/mol.<sup>54</sup> Their methods were used to analyze scaffold II and are described in the next section. Cochran and co-workers argued that the synergistic effects observed by

Smith and Regan did not necessarily imply greater interaction energies, but were related to intrinsic properties of the individual amino acids.<sup>55</sup> Using scaffold I and other constructs, they demonstrated that amino acid preference at one position was the same if the cross-strand position was occupied by aromatic (Tyr and Phe), hydrophobic (Val and Leu), or hydrophilic (Thr) amino acids. Moreover, a linear free-energy relationship was observed between the data sets where deviations from linearity would have indicated specific side-chain–side-chain interactions. We employed the analysis used by Cochran and co-workers to determine if differences in stabilities for scaffold I peptides related to intrinsic properties of the amino acids or side-chain–side-chain interactions.<sup>39,40</sup> This method was particularly applicable to this scaffold, since substitutions at positions  $X_1$  and  $X_2$  are essentially equivalent.<sup>39,40</sup> The  $\Delta G$  of the  $X_1$ -Hfl<sub>2</sub> series was compared to the  $X_1$ -Leu<sub>2</sub> series in Figure 2B. A linear free energy relationship was not observed between the  $X_1$ -Leu<sub>2</sub> and  $X_1$ -Hfl<sub>2</sub> series, as indicated by the  $R^2$  value of 0.312 for a linear fit. HH1 was less stable than LL1 by 190 cal/mol. Both the HL1 and LH1 analogues displayed  $C_{\text{eff}}$  values similar to that of LL1 at 18.75  $\mu\text{M}$  peptide concentration, indicating that the Leu-Hfl interaction or Leu-Leu interaction was more stabilizing than the Hfl-Hfl interaction.

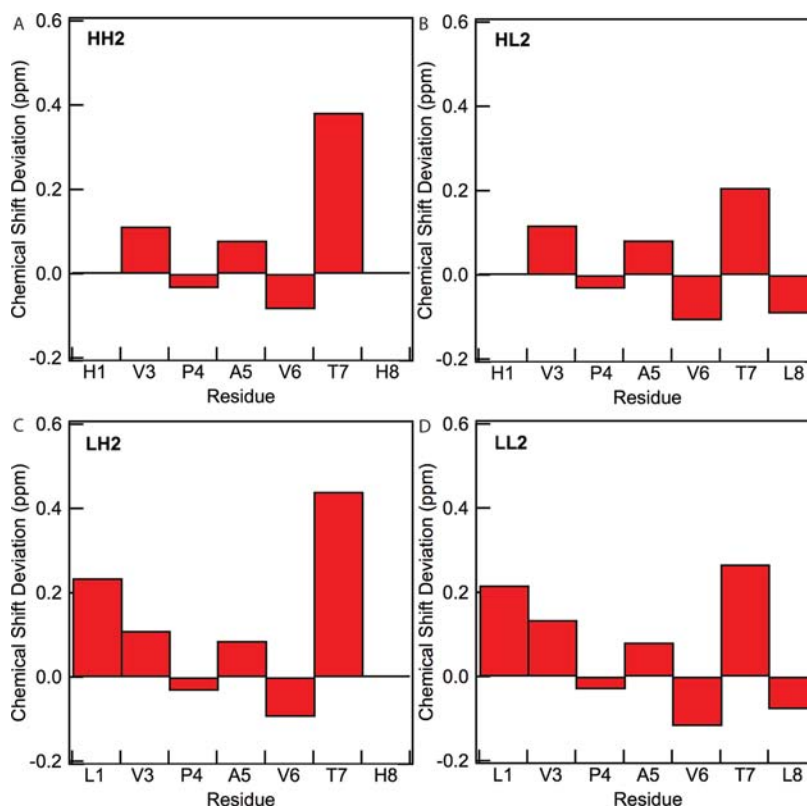


**Figure 5.**  $H_{\alpha}$  Chemical shift deviations from random coil values for (a) HH2, (b) HL2, (c) LH2, and (d) LL2. Chemical shift deviations are not shown for Hfl since insufficient data is available. Conditions: 30%  $CD_3OD$ , 10 mM sodium phosphate, 10 °C, pH 7.0.

While Hfl has a  $\beta$ -sheet propensity similar to that of Leu, it forms weaker interactions with Leu or Hfl. It is possible that the larger aliphatic side chain of Hfl in the disulfide-bound peptide diminishes the stability of HH1. However, large aromatic side chains (in particular Trp) have been previously accommodated in this scaffold resulting in highly stable constructs.<sup>56</sup>

**Determination of Intrinsic Stabilities and Interaction Energies for Scaffold II.** For scaffold II peptides, both the intrinsic stabilities and the interaction energies were calculated using a double mutant analysis method. Intrinsic stability accounts for the contributions of an individual amino acid to the stability of a construct in the absence of interactions with its cross-strand partner.<sup>41</sup> The intrinsic stability for each peptide was calculated from the corresponding peptides that have Gly at the cross-strand position. For example,  $\Delta G^{\circ}$  for LH2 was calculated by summing the stability of LG2 and GH2, then subtracting the stability of GG2. The general equation is:

$$\Delta G^{\circ}_{XY(intrin)} = \Delta G^{\circ}_{X_G} + \Delta G^{\circ}_{G_X} - \Delta G^{\circ}_{GG} \quad (7)$$

As shown in Figure 3B, in the absence of any side-chain–side-chain interactions, HL2 has the highest intrinsic stability. This reflects the preference for Hfl at the N-terminus and Leu at the C-terminus. The interaction energy reflects the contribution of side-chain interactions to the overall stability. Interaction energies between side chains of interest were obtained by subtracting the  $\Delta G^{\circ}_{XY}$  from the intrinsic stability:<sup>41</sup>

$$\Delta G^{\circ}_{XY(inter)} = \Delta G^{\circ}_{XG} - \Delta G^{\circ}_{intrin} \quad (8)$$

As shown in Figure 4B, the interaction energies obtained from scaffold II were consistent with those obtained from scaffold I. Hfl–Hfl side chains exhibit weak interactions, contributing only  $\sim 210$  cal/mol to stability. Leu–Hfl side

chains exhibited modest interactions, from 310 to 350 cal/mol. Leu–Leu interactions were about as strong as Leu–Hfl interactions, contributing 320 cal/mol of stability at 298 K. While the differences between side-chain–side-chain interaction energies were small, these results clearly demonstrate that Hfl interactions were not guided by the hydrophobic effect alone. If this were the case, Hfl–Hfl interactions would have been the strongest rather than the weakest.

**Scaffold II: Measurement of Thermodynamic Parameters in Various Media.** Temperature dependence of hairpin stability has been used to extract the thermodynamic parameters  $\Delta S$ ,  $\Delta H$ , and  $\Delta C_p$  of folding. Searle and co-workers have observed entropy-driven  $\Delta G$  values for 16-residue hairpins, which indicated that the burial of hydrophobic surface area was energetically relevant to hairpin folding.<sup>57,58</sup> The addition of MeOH improved the stability of the constructs, and resulted in enthalpy-driven unfolding.<sup>57</sup> We used a similar strategy to study scaffold II peptides (see SI). With the exception of LH2, the  $\Delta S^{\circ}$  values were negative for these peptides, where the driving force for folding was found in  $\Delta H^{\circ}$  at 298 K. Given the small size of the construct (8 residues) it was not surprising that enthalpic factors (such as H-bonding) play a more significant role in folding. These data were analyzed to determine the contribution of side-chain–side-chain interaction energies to  $\Delta H^{\circ}_{interact}$ ,  $\Delta S^{\circ}_{interact}$ , and  $\Delta C_p_{interact}$ . Interaction entropies, enthalpies, and heat capacities were calculated from the corresponding Gly derivatives as described for  $\Delta G^{\circ}_{XY(inter)}$  in eqs 7 and 8. For these peptides, the magnitude of both the interaction entropy and enthalpy increased with increasing peptide stability.

For each peptide,  $\chi_{\beta}$  was determined in 60% TFE and 90% MeOH (see SI). All peptides displayed increasing  $\chi_{\beta}$  with

Table 1. NMR Structural Data and Refinement Statistics

	LL2	HH2	HL2	LH2
<b>Experimental Restraints</b>				
distance restraints from ROEs/NOEs	48	68	67	77
dihedral angle restraints	10	8	6	9
H-bonding restraints	6	6	6	6
<b>RMS Deviations from Experimental Data</b>				
average distance restraint violation (Å)	0.048 ± 0.013	0.044 ± 0.012	0.032 ± 0.097	0.076 ± 0.007
distance restraint violations >0.5 Å	0	0	0	0
average dihedral angle restraint violations	0.13 ± 0.14	0.21 ± 0.24	0.086 ± 0.075	0.231 ± 0.086
dihedral angle restraint violations >5°	0 ± 0.00	0 ± 0.00	0 ± 0.00	0 ± 0.00
<b>RMS Deviations from Ideal Stereochemistry</b>				
bonds (Å)	0.0033 ± 0.0004	0.0038 ± 0.0004	0.0032 ± 0.0006	0.0051 ± 0.0051
angles (deg)	0.660 ± 0.029	0.771 ± 0.032	0.671 ± 0.028	0.866 ± 0.035
impropers (deg)	0.328 ± 0.057	0.10 ± 0.32	0.37 ± 0.12	0.770 ± 0.057
<b>Ramachandran Analysis of the Structures<sup>a</sup></b>				
residues in favored regions	3	2	2	1
residues in additionally allowed regions	3	2	3	4
residues in generously allowed regions	0	0	0	0
residues in disallowed regions	0	0	0	0
<b>Lennard-Jones Potential Energies</b>				
after annealing (kcal·mol <sup>-1</sup> )	29.9 ± 9.7	11.2 ± 4.5	25.8 ± 4.0	65.6 ± 6.9
ensemble average (kcal·mol <sup>-1</sup> )	5.8 ± 6.1	-13 ± 11	-1.6 ± 6.7	43.9 ± 9.9
<b>Coordinate Precision (Å)</b>				
backbone	0.82 ± 0.32	0.35 ± 0.6	0.44 ± 0.21	0.41 ± 0.17
heavy atoms	1.64 ± 0.39	1.20 ± 0.27	1.35 ± 0.44	1.06 ± 0.23
side-chain precision, residues 1,8 <sup>b</sup>	2.5, 2.4	2.7, 1.1	2.2, 1.1	2.5, 1.3
no. of ensemble structures of 30 where side chains 1 and 8 are <i>very close</i> , <i>close</i> <sup>c</sup>	5, 1	0, 20	21, 9	6, 6

<sup>a</sup>Hfl, Ati, and Pro residues not included in this analysis. <sup>b</sup>The coordinate precision of the heavy atoms in side chains 1 and 8, respectively, after annealing. <sup>c</sup>H–H, H–F, or F–F distances between residues 1 and 8 that are “*very close*” (<3.6 Å apart), and “*close*” (between 3.6 Å and 5.3 Å apart).

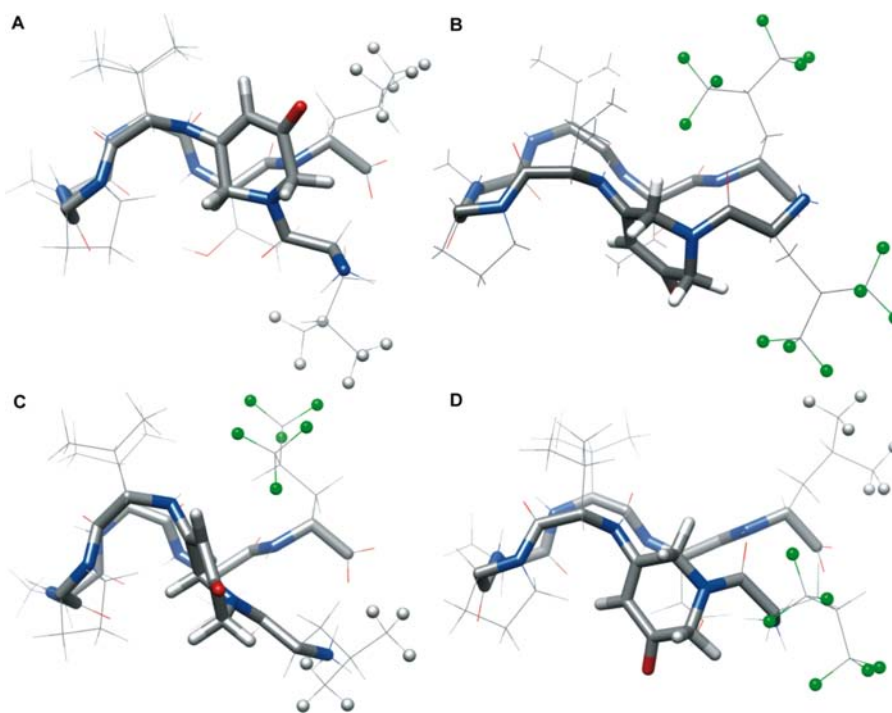


**Figure 6.** NMR solution structures for scaffold II peptides. (A) Average structures for LL2 peptide, (B) HH2, (C) LH2, (D) HL2. N = blue, O = red, C = gray, F = green, H = light gray. The terminal H and F atoms on residues 1 and 8 are depicted as balls. Conditions: 30% CD<sub>3</sub>OD, 10 mM sodium phosphate, 10 °C, pH 7.0.

increasing portions of organic solvents. Furthermore, temperature-dependent CD data were collected in 90% MeOH from 5 to 60 °C and in 60% TFE. These data were fit for the

thermodynamic parameters  $\Delta S^\circ$ ,  $\Delta H^\circ$ , and  $\Delta C_p$  and interaction entropies and enthalpies were calculated (see SI). In all cases  $\Delta G_{XY}^{\circ(inter)}$  was enthalpy-driven at 298 K, and the

more stable peptides had a more negative  $\Delta H^\circ$ . The interaction energies are plotted in Figure 4B. Hfl-Hfl and Hfl-Leu side-chain interactions were stronger in 90% MeOH than in aqueous buffer, whereas Leu-Leu interactions were similar in 90% MeOH to those observed in water. In 60% TFE, Leu-Leu interactions were strengthened, but the effect on Hfl-Hfl and Hfl-Leu interactions was more modest than in 90% MeOH suggesting that fluorinated solvents influence intermolecular interactions in nontrivial ways.

**Scaffold II: Determination of Structure by NMR.** We performed NMR experiments to verify that all peptides form expected  $\beta$ -hairpin structures, and that the side chains of interest interact in the folded form. We chose 30% MeOH for solution conditions as all members of the LL2, HL2, LH2, and HH2 peptide series were well folded as judged from the CD spectra and are present as monomers (as judged from the  $^1\text{H}$  and  $^{19}\text{F}$  NMR spectra). The  $^1\text{H}$  NMR spectra (pH 7.0, 10 °C) showed good dispersion and narrow linewidths, suggesting that the peptides are well-folded and good candidates for structure determination using NMR.

For the four residues with observable NH resonances (residues 3, 6, 7, and 8), the three-bond coupling constants,  $^3J_{\text{HN,H}\alpha}$  were between 8.4 and 9.5 Hz for all peptides, indicating an HN-H $\alpha$  dihedral angle of approximately  $-139^\circ$ , consistent with an antiparallel  $\beta$ -sheet.<sup>59</sup> The formation of  $\beta$ -hairpin structures is supported by the presence of strong H $\alpha$ -NH ROE cross-peaks for residues ( $i, i+1$ ) and cross-strand ROE peaks between residues 2 and 7.<sup>59</sup> All of the peptides showed cross-peaks that included side-chain protons indicating cross-strand interactions. All peptides showed crosspeaks between residues 1 and 6, as expected for a  $\beta$ -hairpin with a type I' or type II' turn.<sup>53</sup> HH2, LH2, and HL2 showed crosspeaks between residues 2 and 7, while HL2 and LL2 showed crosspeaks between residues 1 and 8, indicating that  $\beta$ -hairpin structure extends to the termini of the sequence. H $\alpha$  resonances of residues 1, 3, and 7 were shifted downfield from the resonances expected for a random coil (Figure 5), consistent with  $\beta$ -sheet formation while that of residues 4 and 8 were shifted upfield, consistent with a turn sequence at residue 4 and residue 8 being at the C-terminus.<sup>60</sup> The observation of full intensities for NH resonances at pH 7.0 suggested that these amides were protected from the solvent and consistent with interstrand H-bonding.

Approximately 73 conformational restraints were obtained for each peptide and were input into CNSsolve for structure calculation (Table 1). The resulting statistical analysis of the final structures showed total energies of about 8.8 kcal/mol and the backbone rms deviations of superimposed structures between 0.4 and 0.8 Å. An overlay of the peptide backbones and NMR ensembles for each peptide are provided in the SI. The average structures for the peptides in this series show similar conformations in solution and that the side chains of interest interact (Figure 6). In addition, the side chains alternated from one side of the backbone to the other, consistent with the expected  $\beta$ -hairpin motif. A preservation of conformation in the peptides allowed us to correlate the nature of interactions with fluorinated amino acid side chains to the observed energetic difference in side-chain–side-chain interactions. For each peptide, the hydrophobic side chains of residues one and eight interacted in the ensemble of structures, though not necessarily in the averaged structure. Individual members of all of the ensembles showed significant deviations from the average structure, particularly in residues 1, 2, and 8

that may be in part due to flexibility at the termini. Part of the observed flexibility for residues 1, 2, and 4 is contributed by their lack of NH protons thus missing structural constraints available in the other residues.

In order to evaluate the extent to which side chains 1 and 8 interact, the distances between Leu methyl protons and the analogous fluorines in Hfl were measured in the structural ensembles. A “*very close*” interaction was scored for distances of  $<3.6$  Å, and “*close*” interactions were scored for distances between 3.6 and 5.3 Å. Side-chain interactions were observed in all peptides (Table 1).<sup>39</sup> For LL2, five structures displayed *very close* interactions and one structure had *close* interactions. The interaction distance for the average was only 3.8 Å, indicating that these residues were on average proximal, but more dynamic than in other peptides. For HH2, *close* interactions were observed in 20 structures, but *very close* interactions were not observed suggesting that the larger trifluoromethyl groups tend to be further apart than methyl groups. The interactions were observed for HL2 in all 30 structures, whereas interactions were observed in only 12 structures for LH2. Interestingly, we observed that flexibility is not an indicator of overall stability. LL2 is the most flexible peptide, as judged by the coordinate precision of the backbone atoms (Table 1), yet it is more stable than the more rigid HH2. Notably, LL2 has a favorable energetic contribution from  $T\Delta S^\circ_{\text{interact}}$  while HH2 does not (see SI), illustrating the complex interplay of entropic and enthalpic parameters in determining interaction energies and peptide stabilities.

## DISCUSSION

When considering conformational stabilities of peptides, steric clashes, backbone perturbations, inductive effects,<sup>22,61</sup> and the interaction energies of proximal side chains all play an important role. We examined two series of peptides to demonstrate the effect of side-chain interactions on conformational stability. We chose to study hairpin constructs, where side chains are partially solvent-exposed, and thus able to accommodate larger groups. We demonstrated by NMR that the substitution of Leu with Hfl does not significantly perturb the peptide backbone and further confirmed that side-chain sterics are not an issue for scaffold II peptides. We found similar results when substitutions were performed at non-hydrogen bonded positions on a peptide (scaffold I) and the N- and C-termini of a peptide (scaffold II). This demonstrates that the observed differences in interaction energies are not the result of inductive effects that may perturb hydrogen bonding of backbone atoms, as these effects would be structure-specific. Therefore, our study is directly able to compare interactions of Leu and Hfl.

One might expect that the Hfl-substituted constructs would be more stable than Leu-substituted constructs, since Hfl is more hydrophobic. However, we found that Hfl-Hfl interactions were weaker than Leu-Leu or Leu-Hfl interactions. This demonstrates that the effect of substitution of hydrogen with fluorine depends upon the subtle interplay of polarizability, dipolar interactions, and hydrophobicity. It is possible that the low polarizability relative to volume of  $\text{CF}_3$  vs  $\text{CH}_3$  influences the interaction energies of Hfl.<sup>62</sup> We also found that the Hfl-Leu interface had an interaction energy that was similar to the Leu-Leu interface in water. It is possible that this interaction is influenced by dipolar interactions, since the C–F bond ( $\mu = 1.85$  D), and the C–H bond ( $\mu = 0.4$  D) have dipoles in opposite directions. Dipolar interactions must also be



considered when examining solvent effects, as dipolar interactions are often magnified with decreasing solvent polarity.<sup>63</sup> The differences observed between interaction energies in 90% MeOH and 60% TFE for each of the side-chain pairs serve only to highlight the complexity of these interactions.

In this construct, the side chains are not well-shielded from water in the folded state. In contrast, previous work demonstrated that fluorinated amino acid substitutions into coiled coils were generally stabilizing. An understanding of how these interactions were altered by the hydrophobicity of the medium directs us toward methods for targeting membrane-bound proteins or hydrophobic binding pockets.

This construct may also be used to probe other molecular interactions, such as interactions of Hfl with aromatic residues. Information on these interactions may have broader implications in drug design and improve our fundamental understanding of interactions involving fluorinated compounds.

## CONCLUSIONS

A methyl to trifluoromethyl substitution is frequently used in pharmaceutical design, as this substitution can greatly alter the specificity and potency of a drug. For example, the changing the trifluoromethyl group on fluoxetine (Prozac) to a methyl group leads to a 26-fold decrease in specificity.<sup>64</sup> We have evaluated the interaction energies of Hfl-Hfl, Leu-Hfl and Leu-Leu in two different scaffolds to analyze the interactions of trifluoromethyl with both hydrocarbon and fluorocarbon groups in  $\beta$ -hairpin motifs. Our results suggest that the binding of methyl to trifluoromethyl groups depend on more than just size and hydrophobicity and advance our understanding of interactions of fluorinated amino acids in biological contexts.

## ASSOCIATED CONTENT

### Supporting Information

Synthetic methods, accompanying analytical data, thermodynamic analysis, NMR fitting procedures, CD spectra and fitting curves, and HPLC traces. This material is available free of charge via the Internet at <http://pubs.acs.org>.

## AUTHOR INFORMATION

### Corresponding Author

[jim.baleja@tufts.edu](mailto:jim.baleja@tufts.edu) (J.D.B.); [krishna.kumar@tufts.edu](mailto:krishna.kumar@tufts.edu) (K.K.).

### Present Address

<sup>†</sup>University of Illinois Chicago, Department of Chemistry, 845 West Taylor Street, MC 111, Chicago, IL 60607, United States.

### Notes

The authors declare no competing financial interest.

## ACKNOWLEDGMENTS

This work was supported by the National Institutes of Health (GM65500 to K.K.). The ESI-MS and NMR facilities at Tufts are supported by the NSF (0320783 and 0821508). G.C. was supported as a GAANN fellow for part of this work (US Department of Education). We thank Vijay K. Murthy, Ragnhild Whitaker, and Yuqi Liu for helpful discussions.

## REFERENCES

- (1) Muller, K.; Faeh, C.; Diederich, F. *Science* **2007**, *317*, 1881–1886.
- (2) Yoder, N. C.; Yuksel, D.; Dafik, L.; Kumar, K. *Curr. Opin. Chem. Biol.* **2006**, *10*, 576–583.

- (3) Dafik, L.; d'Alarcao, M.; Kumar, K. *J. Med. Chem.* **2010**, *53*, 4277–4284.
- (4) Riess, J. G. *Tetrahedron* **2002**, *58*, 4113–4131.
- (5) Meng, H.; Clark, G. A.; Kumar, K. In *Fluorine in Bioorganic and Medicinal Chemistry*; Ojima, I., Taguchi, T., Eds.; Blackwell-Wiley Publishing: New York, 2009.
- (6) Scott, R. L. *J. Am. Chem. Soc.* **1948**, *70*, 4090–4093.
- (7) Hildebrand, J. H.; Cochran, D. R. F. *J. Am. Chem. Soc.* **1949**, *71*, 22–25.
- (8) Santaella, C.; Vierling, P.; Riess, J. G.; Gulikkrzywicki, T.; Gulik, A.; Monasse, B. *Biochim. Biophys. Acta* **1994**, *1190*, 25–39.
- (9) Biffinger, J. C.; Kim, H. W.; DiMaggio, S. G. *ChemBioChem* **2004**, *5*, 622–627.
- (10) Bilgicer, B.; Xing, X.; Kumar, K. *J. Am. Chem. Soc.* **2001**, *123*, 11815–11816.
- (11) Bilgicer, B.; Kumar, K. *Tetrahedron* **2002**, *58*, 4105.
- (12) Widom, B.; Bhimalapuram, P.; Koga, K. *Phys. Chem. Chem. Phys.* **2003**, *5*, 3085–3093.
- (13) Bilgicer, B.; Kumar, K. *Proc. Natl. Acad. Sci. U.S.A.* **2004**, *101*, 15324–15329.
- (14) Bilgicer, B.; Fichera, A.; Kumar, K. *J. Am. Chem. Soc.* **2001**, *123*, 4393–4399.
- (15) Stevens, M. M.; Flynn, N. T.; Wang, C.; Tirrell, D. A.; Langer, R. *Adv. Mater.* **2004**, *16*, 915–918.
- (16) Son, S.; Tanrikulu, I. C.; Tirrell, D. A. *ChemBioChem* **2006**, *7*, 1251–1257.
- (17) Wang, P.; Tang, Y.; Tirrell, D. A. *J. Am. Chem. Soc.* **2003**, *125*, 6900–6906.
- (18) Niemi, A.; Tirrell, D. A. *J. Am. Chem. Soc.* **2001**, *123*, 7407–7413.
- (19) Tang, Y.; Ghirlanda, G.; Vaidehi, N.; Kua, J.; Mainz, D. T.; Goddard, W. A.; DeGrado, W. F.; Tirrell, D. A. *Biochemistry* **2001**, *40*, 2790–2796.
- (20) Gao, J. M.; Qiao, S.; Whitesides, G. M. *J. Med. Chem.* **1995**, *38*, 2292–2301.
- (21) (a) Molski, M.; Goodman, J.; Craig, C.; Meng, H.; Kumar, K.; Schepartz, A. *J. Am. Chem. Soc.* **2010**, *132*, 3658–3659. (b) Buer, B. C.; Meagher, J. L.; Stuckey, J. A.; Marsh, E. N. G. *Proc. Natl. Acad. Sci. U.S.A.* **2012**, *109*, 4810–4815.
- (22) Krishnamurthy, V. M.; Bohall, B. R.; Kim, C. Y.; Moustakas, D. T.; Christianson, D. W.; Whitesides, G. M. *Chem.—Asian J.* **2007**, *2*, 94–105.
- (23) Lee, A.; Mirica, K. A.; Whitesides, G. M. *J. Phys. Chem. B* **2011**, *115*, 1199–1210.
- (24) Gottler, L. M.; de la Salud-Bea, R.; Marsh, E. N. G. *Biochemistry* **2008**, *47*, 4484–4490.
- (25) Meng, H.; Krishnaji, S. T.; Beinborn, M.; Kumar, K. *J. Med. Chem.* **2008**, *51*, 7303–7307.
- (26) Meng, H.; Kumar, K. *J. Am. Chem. Soc.* **2007**, *129*, 15615–15622.
- (27) Chiu, H. P.; Kokona, B.; Fairman, R.; Cheng, R. P. *J. Am. Chem. Soc.* **2009**, *131*, 13192–13193.
- (28) Senguen, F. T.; Doran, T. M.; Anderson, E. A.; Nilsson, B. L. *Mol. Biosyst.* **2011**, *7*, 497–510.
- (29) Senguen, F. T.; Lee, N. R.; Gu, X. F.; Ryan, D. M.; Doran, T. M.; Anderson, E. A.; Nilsson, B. L. *Mol. Biosyst.* **2011**, *7*, 486–496.
- (30) Tatko, C. D.; Waters, M. L. *J. Am. Chem. Soc.* **2002**, *124*, 9372–9373.
- (31) Tsou, L. K.; Tatko, C. D.; Waters, M. L. *J. Am. Chem. Soc.* **2002**, *124*, 14917–14921.
- (32) Griffiths-Jones, S. R.; Maynard, A. J.; Searle, M. S. *J. Mol. Biol.* **1999**, *292*, 1051–1069.
- (33) Gordon, N. C.; Pan, B.; Hymowitz, S. G.; Yin, J. P.; Kelley, R. F.; Cochran, A. G.; Yan, M. H.; Dixit, V. M.; Fairbrother, W. J.; Starovasnik, M. A. *Biochemistry* **2003**, *42*, 5977–5983.
- (34) Skelton, N. J.; Chen, Y. M.; Dubree, N.; Quan, C.; Jackson, D. Y.; Cochran, A.; Zobel, K.; Deshayes, K.; Baca, M.; Pisabarro, M. T.; Lowman, H. B. *Biochemistry* **2001**, *40*, 8487–8498.

- (35) Fairbrother, W. J.; Christinger, H. W.; Cochran, A. G.; Fuh, C.; Keenan, C. J.; Quan, C.; Shriver, S. K.; Tom, J. Y. K.; Wells, J. A.; Cunningham, B. C. *Biochemistry* **1998**, *37*, 17754–17764.
- (36) Wiesmann, C.; Christinger, H. W.; Cochran, A. G.; Cunningham, B. C.; Fairbrother, W. J.; Keenan, C. J.; Meng, G.; de Vos, A. M. *Biochemistry* **1998**, *37*, 17765–17772.
- (37) Butterfield, S. M.; Sweeney, M. M.; Waters, M. L. *J. Org. Chem.* **2005**, *70*, 1105–1114.
- (38) Butterfield, S. M.; Cooper, W. J.; Waters, M. L. *J. Am. Chem. Soc.* **2005**, *127*, 24–25.
- (39) Cochran, A. G.; Tong, R. T.; Starovasnik, M. A.; Park, E. J.; McDowell, R. S.; Theaker, J. E.; Skelton, N. J. *J. Am. Chem. Soc.* **2001**, *123*, 625–632.
- (40) Russell, S. J.; Cochran, A. G. *J. Am. Chem. Soc.* **2000**, *122*, 12600–12601.
- (41) Phillips, S. T.; Piersanti, G.; Bartlett, P. A. *Proc. Natl. Acad. Sci. U.S.A.* **2005**, *102*, 13737–13742.
- (42) Phillips, S. T.; Blasdel, L. K.; Bartlett, P. A. *J. Am. Chem. Soc.* **2005**, *127*, 4193–4198.
- (43) Phillips, S. T.; Piersanti, G.; Ruth, M.; Gubernator, N.; van Lengerich, B.; Bartlett, P. A. *Org. Lett.* **2004**, *6*, 4483–4485.
- (44) Phillips, S. T.; Rezac, M.; Abel, U.; Kossenjans, M.; Bartlett, P. A. *J. Am. Chem. Soc.* **2002**, *124*, 58–66.
- (45) Haggmann, W. K. *J. Med. Chem.* **2008**, *51*, 4359–4369.
- (46) Brunger, A. T.; Adams, P. D.; Clore, G. M.; DeLano, W. L.; Gros, P.; Grosse-Kunstleve, R. W.; Jiang, J. S.; Kuszewski, J.; Nilges, M.; Pannu, N. S.; Read, R. J.; Rice, L. M.; Simonson, T.; Warren, G. L. *Acta Crystallogr., Sect. D: Biol. Crystallogr.* **1998**, *54*, 905–921.
- (47) Kotz, J. D.; Bond, C. J.; Cochran, A. G. *Eur. J. Biochem.* **2004**, *271*, 1623–1629.
- (48) Russell, S. J.; Blandl, T.; Skelton, N. J.; Cochran, A. G. *J. Am. Chem. Soc.* **2003**, *125*, 388–395.
- (49) Dyson, H. J.; Rance, M.; Houghten, R. A.; Lerner, R. A.; Wright, P. E. *J. Mol. Biol.* **1988**, *201*, 161–200.
- (50) Minor, D. L.; Kim, P. S. *Nature* **1994**, *367*, 660–663.
- (51) Minor, D. L.; Kim, P. S. *Nature* **1994**, *371*, 264–267.
- (52) Zhang, H. S.; Pan, J.; Hogen-Esch, T. E. *Macromolecules* **1998**, *31*, 2815–2821.
- (53) Syud, F. A.; Stanger, H. E.; Gellman, S. H. *J. Am. Chem. Soc.* **2001**, *123*, 8667–8677.
- (54) Smith, C. K.; Regan, L. *Science* **1995**, *270*, 980–982.
- (55) Distefano, M. D.; Zhong, A.; Cochran, A. G. *J. Mol. Biol.* **2002**, *322*, 179–188.
- (56) Cochran, A. G.; Skelton, N. J.; Starovasnik, M. A. *Proc. Natl. Acad. Sci. U.S.A.* **2001**, *98*, 5578–5583.
- (57) Baldwin, R. L. *Proc. Natl. Acad. Sci. U.S.A.* **1986**, *83*, 8069–8072.
- (58) Maynard, A. J.; Sharman, G. J.; Searle, M. S. *J. Am. Chem. Soc.* **1998**, *120*, 1996–2007.
- (59) Wüthrich, K. *NMR of Proteins and Nucleic Acids*; Wiley: New York, 1986.
- (60) Williamson, M. P. *Biopolymers* **1990**, *29*, 1428–1431.
- (61) Gorske, B. C.; Blackwell, H. E. *J. Am. Chem. Soc.* **2006**, *128*, 14378–14387.
- (62) Dunitz, J. D. *ChemBioChem* **2004**, *5*, 614–621.
- (63) Weber, G. *Protein Interactions*; Chapman Hall: New York, 1992.
- (64) Wong, D. T.; Bymaster, F. P.; Engleman, E. A. *Life Sci.* **1995**, *57*, 411–441.